Hindawi
Advances in Materials Science and Engineering
Volume 2022, Article ID 2530707, 11 pages
https://doi.org/10.1155/2022/2530707

Research Article

Thermal Analysis of Ni-Cu Alloy Nanocomposites Processed by Sand Mold Casting

J. Kumaraswamy,[1] **Vidyasagar Shetty**,[2] **S. Sanman**,[3] **Premkumar Naik**,[4] **Shabari Shedthi**,[5] **C. Gnanavel**,[6] **and Ibsa Neme Mogose**[7]

[1]*Department of Mechanical Engineering, RL Jalappa Institute of Technology (Visvesvaraya Technological University Belagavi, Doddaballapur 561203, Karnataka, India*
[2]*Department of Mechanical Engineering, NMAM Institute of Technology- Affiliated to NITTE (Deemed to be University), Nitte 574110, Karnataka, India*
[3]*Department of Mechanical Engineering, Acharya Institute of Technology, Bengaluru 560107, Karnataka, India*
[4]*Department of Mechanical Engineering, AMC Engineering College, Bengaluru 560083, Karnataka, India*
[5]*Department of Computer Science and Engineering, NMAM Institute of Technology- Affiliated to NITTE (Deemed to be University), Nitte 574110, Karnataka, India*
[6]*Department of Mechanical Engineering, Vels Institute of Science, Technology and Advanced Studies, Chennai 600 117, India*
[7]*Department of Chemical Engineering, College of Biological and Chemical Engineering, Addis Ababa Science and Technology University, Addis Ababa, Ethiopia*

Correspondence should be addressed to Vidyasagar Shetty; vidyasagar.shetty@gmail.com and Ibsa Neme Mogose; ibsa.neme@aastu.edu.et

Received 6 May 2022; Accepted 24 June 2022; Published 19 August 2022

Academic Editor: V. Vijayan

Copyright © 2022 J. Kumaraswamy et al. This is an open access article distributed under the Creative Commons Attribution License, which permits unrestricted use, distribution, and reproduction in any medium, provided the original work is properly cited.

Ni-Cu based alloy metal matrix nanocomposites are in great demand for advanced technological applications due to their high temperature, strength, and better thermal properties. The aim is to investigate the thermal conductivity and coefficient of thermal expansion of the nickel based alloy nanocomposites reinforced with titanium dioxide (TiO_2) which varies from 3 to 12 weight % nanoparticulates (45 to 60 nm). The thermal conductivity was measured using a comparative cut bar method (ASTM E1225), and thermal expansion was analyzed using a push-rod dilatometer method (ASTM E228). From experimentation, it was observed that thermal conductivity of the nanocomposites activity increases with inclusion of the nanoparticles up to 9 weight % after descent due to the temperature effects in nanocomposites, and thermal expansion of the nanocomposites decreases with addition of the nanoparticles up to 9 weight % and further rises marginally due to ductility of composites. Due to the incorporation of hard ceramic particles into the matrix, the composites' thermal conductivity increases to 57.42 W/m ℃, and their thermal expansion decreases to 12×10^{-6}. Nickel alloys are widely used in marine, automotive, valve, pump, and aircraft applications.

1. Introduction

Nickel (Ni) has made significant contributions in its elementary form with other materials and promises to provide materials for a much more demanding future. Nickel is a multifaceted metal with a variety of other metals. Nickel alloys are employed in different applications due to their ability to withstand harsh working conditions such as high temperatures, corrosion, wear strength, intense friction, metallurgical durability, solderability, and strength. The high corrosion and heat resistance are required in most applications, such as aircraft applications, nuclear power systems, and automotive and petrochemical exhaust valves [1–5]. As composite prices come down and design suppleness improves, particle reinforced composites like hard ceramic particulates and fiber reinforced composites like fiberglass

and carbon fiber open up new design opportunities for engineers. MMCs never rust, regardless of the climate (however they are predisposed to corrosion when fused to metal parts). Composites have less fracture strength than metals. Their high dimensional constancy lets them maintain their shape in all conditions (hot/cold, wet/dry). This makes them popular materials for outdoor constructions such as turbine blades. Engineers prefer composites over traditional materials to save money on repairs and ensure long-term consistency, which is a big deal for structures that are meant to last a long time. The use of MMCs will be a preferable option in certain situations, and the use of materials will depend on considerations such as working time, number of pieces to be made, size of the form, the likely savings on assembly costs on the expertise and skills of the manufacturer in choosing the optimal potential in MMCs [6, 7]. Thermal conductivity of a composite material depends on the fiber, resin materials, fiber volume fraction, fiber orientation, direction of heat flow, and operating temperature. Applications such as aerospace, automotive industry, building materials, power generation, glass industry, energy industries, or ceramic commercial ventures require exact information about the thermal conductivity of the materials used [8–12]. Thermal tests were carried out on a nickel alloy (ASTM A494 M) reinforced with fused SiO_2, with particle sizes ranging from 80 to 120 μm and SiO_2 additions ranging from 3 to 12 wt. % in 3 wt. % steps. Chilled MMCs were solidified using a copper chill of 25 mm thickness to investigate the effect of chilling on thermal characteristics. Thermal properties in chilled MMCs decreased notably as SiO_2 content increased [13–15]. Aluminum-silicon hybrid composites reinforced with silicon carbide and graphite particles were produced using liquid phase particle mixing (melt stirring). Thermal expansion and thermal conductivity of hybrid composites with varying graphite contents (5, 7.5, and 10 wt. %) and silicon carbide particle sizes (45 μm and 53 μm) were investigated. The results showed that raising the graphite content improved dimensional stability, but the thermal expansion behaviors of the 45 μm and 53 μm silicon carbide reinforced composites were not substantially different. Since the graphite portion was enriched, it reduced the thermal conductivity of hybrid composites [16]. The study analyzed Al6061 SiC and Gr hybrid composites at 2.5%, 5%, 7.5%, and 10%. SEM and EDAX, which are useful for thermal characterization and analysis of composite materials, were used to research these hybrid composites. The thermal conductivity of hybrid composites with varying percentages of lower proportional reinforcements was demonstrated. The coefficient of thermal expansion (CTE) is the most important factor affecting the composite dimensional stability. The material changes shape proportional to the amount of temperature change multiplied by its coefficient of thermal expansion when subjected to a thermal load. For each degree of temperature change, the CTE shows how much materials change shape. In small temperature ranges, CTE can be considered to be linear. Over small temperature ranges, the thermal expansion of normal dimensional structures is proportional to the temperature rise. Thermal expansion is used in the manufacture of thermometers using pneumatic strips, but it can cause dangerous stress when the structural part is heated and held at a constant rate. Between the matrix phase and the reinforcement phase, there was always a state of micro tension. The difference in thermal expansion between individual phases influenced the strength properties and failure modes in a roundabout way [5, 17, 18]. The thermal expansion behaviour of aluminium matrix composites reinforced with fused quartz nanoparticles were evaluated and compared to theoretical models from 30 to 300 ˚C. The results showed that the nanoparticle volume fraction had a substantial impact on the composite thermal expansion activity. The coefficient of thermal expansion (CTE) of composites with a lower nanoparticle volume fraction is determined by a stress relaxation mechanism. A random network of aggregated clusters made of cristobalite, tridymite, and quartz with nanometer-scale measurements produces the hysteresis between the heating and cooling cycles, as well as the preservation of residual [19]. The CTE of pure aluminum and aluminum composites reinforced with fly ash particles of average size 125 μm. Pressure infiltration technique was used to create three forms of composites at applied pressures and infiltration times of 35 kPa for 3 minutes, 35 kPa for 7 minutes, and 62 kPa for 7 minutes. Fly ash cenosphere volume fractions in the composites were about 65%. The CTE of fly ash cenospheres was calculated to be 6.1×10^{-6}/˚C theoretically. The composite CTE was estimated to be between 13.1×10^{-6} and 11×10^{-6}/˚C, which was lower than pure aluminum (25.3×10^{-6}/˚C). The CTE of the composites was influenced by infiltration processing conditions. In pure Al matrix, the presence of fly ash cenospheres reduced CTE [20]. Energy Dispersive Spectroscopy (EDS) is primarily used to provide semiquantitative results in qualitative material research. An EDS device is usually included with a SEM instrument to enable chemical analysis of features seen on the display. In failure analysis cases where spot analysis is critical to draw a reliable conclusion, simultaneous SEM and EDS analysis are beneficial. Secondary and backscattered electrons are used to shape a picture needed for morphological analysis, and X-rays are used to identify and quantify chemicals present in observable concentrations in a SEM/EDS framework [21–27]. The technique of X-ray diffraction is used to analyze crystal structures and atomic spacing. This method uses monochromatic X-rays and a crystalline sample to create constructive interference. X-rays from a cathode ray tube are filtered to create monochromatic radiation, collimated to concentrate them and guided toward the sample in this technique. Constructive interference of a monochromatic beam of X-rays distributed at various angles from each range of lattice planes in the sample produces diffraction peaks. The distribution of atoms within the lattice determines peak intensities. As a result, the fingerprint of periodic atomic arrangements in a given material is formed by X-ray diffraction patterns [28]. In the present work, the Ni-Cu alloy/TiO_2 hybrid composites were established with the help of a sand molding process to study the microstructure and thermal characteristics. In this study, an induction furnace is utilized to prepare the nickel alloy-based metal matrix composites with variable weight fractions of 0, 3, 6, 9, and 12% titanium dioxide (TiO_2) nanoparticles. Based on the ASTM standard, the manufactured nickel-copper A494 M alloy-based metal

matrix composites endure the evaluation of microstructure and thermal characteristics. In this study, thermal properties like thermal conductivity and thermal expansion analysis are performed on a different temperature conditions.

2. Materials and Method

2.1. Selection of Materials. In the present work, ASTM A494 M35-1 (Monel-400) Ni-Cu alloys were selected as matrix material for the fabrication of metal matrix composites. In addition to the salt and caustic solutions, the alloy is resistant to seawater and steam at high temperatures. The Ni-Cu alloy is a solid solution alloy, which can be treated only by cold action. These nickel alloys possess properties of good wear resistance, excellent weldability, and high strength. The low rate of corrosion flowing rapidly in seawater or saltwater, along with excellent resistance to stress-induced corrosion in most freshwater and its tolerance to a range of corrosive environments, has resulted in its extensive use in marine applications. Table 1 displays the chemical composition of alloys made from nickel. The titanium dioxide (TiO_2) was selected as reinforcement; it is the ninth most regular component in the covering of the Earth and is a mineral found normally in plants and creatures. Titanium responds normally with oxygen to frame titanium oxides, ordinarily found in crude materials, unique residue, sand, and soil. Pure titanium dioxide is a fine white powder which gives splendid white shading. For a century, titanium dioxide has been utilized in an assortment of mechanical and customer merchandise [29–31].

Presently, more research is focused on incorporating nanolevel particles into composites. Based on literature survey, a decrease in particle size increases the production difficulty several times. The existing technology cannot produce microparticles in excess of 12 vol. % due to exponential increase in the surface of the particle for wetting and an increase in number of particles per vol. % to that of micron sized particle which in turn results in undesirable clustering of particles. In the present investigation, the Ni-Cu alloy metal matrix composites were fabricated using an induction furnace linked to a mechanical motor with different weight percentages of 0, 3, 6, 9, and 12% titanium dioxide nanoparticulates in steps of 3 wt. % stages. Scanning Electron Microscope (SEM) images of TiO_2 reinforced particles are shown in Figure 1.

2.2. Sand Mold Casting of MMCs. In the present study, the nickel based alloy metal matrix composites (MMCs) were fabricated using an induction furnace linked to a mechanical motor with different weight percentage of 3 to 12 wt. % titanium dioxide in steps of 3 wt. % stages. Compositions of metal matrix composites (MMCs) for different specimens are indicated in Table 2. Conventional sand molds were used to prepare molding with dimensions of $160 * 40 * 25$ mm and $64 * 44 * 30$ mm using wooden patterns. Silica sand was poured into the acclimatization box and manually hammed with wooden mallets. Then, the mold cavity is primed with zircon and painted to enhance surface finish, and it also prevents the fusion of high-temperature sand particulates. As per the American Foundry Society (AFS), model of the size of 160 mm × 40 mm × 25 mm and a teak model of 64 mm × 44 mm × 30 mm were used with standard style suits. The mold was prepared using 5% bentonite silica sand as a binder and 5% humidity. The induction furnace preheated to 600°C and the base metals along with reinforcing materials were melted in the induction furnace. It was heated up to 1455°C melting temperatures, and reinforcements were preheated at 600°C to remove surface impurity and increase reinforcement wettability. A mechanical stirrer was used to get homogenous mixing of MMCs by adding reinforcement from 3 weight % to 12 weight % in steps of weight 3%. Degassing pills were added to the matrix material in order to remove the entrapped air from the melt. When the heat in the induction furnace reached 1455°C in the matrix, the preheated reinforcement was added with different weight % to the vortex of a Ni-Cu alloy. The stirring was then done using a carbide-coated stirrer at a speed of 200 rpm for 10 minutes to ensure the reinforcement

Table 1: Elemental composition of ASTM A494 M35-1 nickel alloy.

Elements	Percentage
Nickel	63 min
Copper	33 max
Iron	3.5 max
Manganese	1.5 max
Silicon	1.25 max
Columbium (niobium)	0.5 max
Carbon	0.35 max
Phosphorus	0.03 max
Sulfur	0.02 max

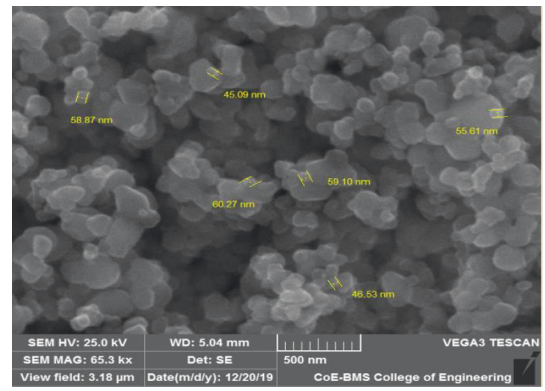

Figure 1: SEM images of TiO_2 nanoparticles.

Table 2: Composition of MMCs for different specimens.

Specimen	Composition weight percentage	
	Ni-Cu alloy	Titanium dioxide (TiO_2)
A	100	—
B	91	9
C	82	9
D	73	9
E	64	9

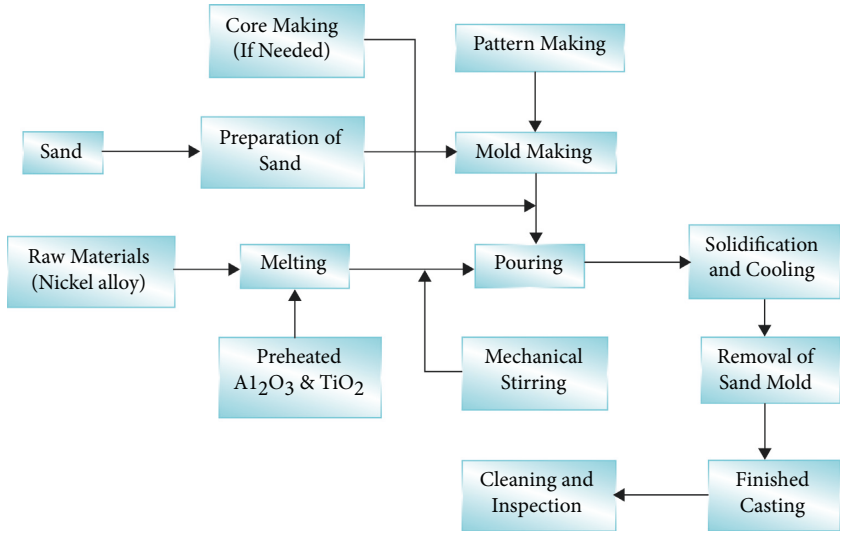

Figure 2: Procedural steps for sand mold casting.

distribution is concerned. The prepared solubility was then poured into the mold and allowed to cool to room temperature to solidify. After 12 hours, sand mold was removed to obtain the final casting, which was subsequently cleaned and taken for inspection as shown in Figure 2. The process parameters employed during the preparation of the composite are shown in Table 3.

Table 3: Process parameters of the composite.

Sl. no.	Parameter	
(1).	Stirring speed	50–150 rpm
(2).	Stirring time	5–15 min
(3).	Temperature of the melt	1400–1500°C
(4).	Preheating temperature of reinforcement particles	600°C
(5).	Pouring temperature of the melt	1455°C

3. Testing of Composites

The composite test samples were prepared as per the ASTM standards and tested for microstructure and thermal characteristics.

3.1. Microstructural Characteristics. Microstructural examination was made by Scanning Electron Microscope (SEM) to examine the dispersion of the reinforcement nanoparticles in composites. Metallographic preparation of sample polishing was adopted for conducting microstructure study. The sample obtained in the bench milling machine was milled to clean burrs and polish the surfaces using the 400, 600, 800, and 1000 grain size sand sheets. The polished samples obtained according to ASTM E3-11 standards were cleaned using a Kroll reagent (92 ml of distilled water, 6 ml of nitric acid, and 2 ml of hydrofluoric acid) for 10–20 seconds before scanning using Nikon-ECLIPSE LV150 optical metallurgical microscope, Japan.

3.2. Thermal Conductivity and Expansion. Thermal conductivity is used to calculate temperature variations and heat flux. Absolute measurement is when heat flux is measured directly (for example, by calculating the electrical power being routed into the heater). Heat flux is referred to as comparative when it is determined indirectly (by comparison). The composite material thermal conductivity then rises gradually as the temperature rises. As a result, thermal conductivity is suitable for engineering purposes. The thermal conductivity was measured using a comparative cut bar (ASTM E1225 Test Method). The measurement principle is to pass heat flux between known and unknown samples and then compare the inversely proportional thermal gradients. To account for minor heat losses that are difficult to extract, the unknown sample is often sandwiched between two known samples, referred to as "the references." Thermal conductivity of the unknown sample K_s can be determined by the following equation:

$$K_S = K_r \times \frac{L_S}{L_r} \times \left[\frac{(T_1 - T_2) + (T_3 - T_4)}{2(T_2 - T_3)}\right] \frac{W}{M}\,℃, \quad (1)$$

where K_r is the thermal conductivity of the reference sample in W/m℃, L_s is the length of the specimen in mm, and L_r is the length of the reference sample in mm, with the thermal conductivity of the reference materials being = 130 W/m℃. The measurement of linear thermal expansion of solid materials was done by the standard test method using the push-rod dilatometer (ASTM E228). This technique was used to determine the CTE of rigid solids like metals, refractories, ceramics, glasses, graphite, cements, rocks, minerals, and different types of composites. Thermal expansion tests were carried out with a quality dilatometer (Anter-Unitherm Model 1161 V) for the prepared samples (8 mm diameter × 50 mm length). Each and every testing trial was conducted in a temperature range of 50 to 300 °C under protected, unrestricted conditions. The warming and cooling rates were measured 5 °C/min and were continuously limited by a PC-based information data acquisition

device. Figure 3shows the position of the composite sample including reference specimen. The thermal analysis of test specimen is shown in Figure 4.

4. Results and Discussion

4.1. Microstructure Analysis. Figures 5(a) and 5(b) show the microscopic images of nickel alloy and Ni-based (Ni-alloy/TiO_2) matrix composites. Figure 5(a) shows the microscopic image of unreinforced Ni-alloy indicating the distribution of nickel in dendrite arms and in interdendritic regions of nickel-copper alloy solidified under production condition. From Figure 5(b), it is observed that the transparent dark gray region is the solid solution for the nickel alloy reinforcement particles, and the remaining region is the matrix. The obvious ambiguous spots in the picture illustrate the accumulation of TiO_2 nanoparticles in the microscopic structure. Heterogeneous solid solutions are formulated to facilitate the formation of a fine dendrite structure in the entire metal matrix, improving the bonding and polishing process of powder. This is due to the 10-minute stirring period during the casting process, which uniformly distributes the reinforcing particles in the metal matrix with minimal mass and minimum structure. Contrasting the tiny pictures of the hybrid composite with the Ni combination, we can see the detachment at the distinction interims in the two examples; however,dendrite a safe distancethe dendrite structure in the composite was seen as lower than it was because of an obstacle of the width of the fortification particles during hardening. For the most part, because of the renovated grain structure, there is a significant improvement in mechanical properties, while the expansion in the division is fundamental because of the nearness of support particles which reduce stretching properties while improving load ability.

SEM micrograph recommends trace amounts of filler materials in metal matrix composite demonstrating fracture resistance because of better dispersal of basic materials in comparison to the pristine epoxide composite. Blended analysis of SEM-EDX aids in identifying the effect of chemical reaction on the microscopic structure of the composite. Particle added substance tests show that mechanical properties strengthen because of the heterogeneous nucleation of the strengthening globules, with the production of a fragile structure as shown in Figure 6.

4.2. Thermal Conductivity. In composite material, investigation of thermal conductivity was estimated at various temperatures for various nickel combinations, with varied rates of steady weight of TiO_2. The fundamental aftereffect of the test was that nickel combination thermal conductivity with the expansion of nickel composite (base metal) and TiO_2 increases continually with increasing temperature up to 9% of weight. With the expansion in weight level of TiO_2, the thermal conductivity increases as the temperature rises. Figure 7 shows that thermal conductivity for the Ni composite changes at varied temperature of 47.399 W/m°C without reinforcement. The highest thermal conductivity for

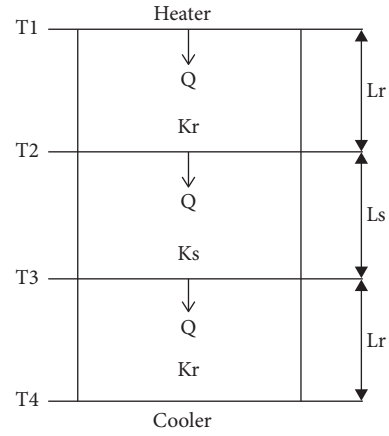

Figure 3: Positions of the reference and test specimens for thermal conductivity.

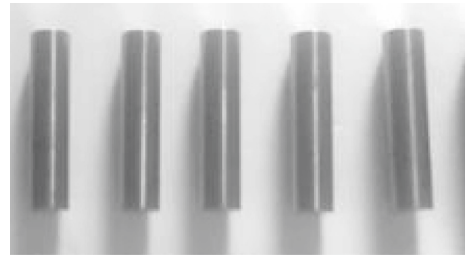

Figure 4: Specimens of the thermal analysis.

the Ni junction structure was 57.42 W/m°C in 9 wt. % of TiO_2 composite materials, while basic thermal conductivity was 47.39 W/m°C. Despite the temperature, thermal conductivity constantly increased up to 9 weight percentage of TiO_2 with increasing reinforcement content from the plot. For the content of reinforcements greater than 9% wt., thermal conductivity decreased despite aggregation of reinforcements (as evident from microstructural observation). Figure 8 illustrates the thermal conductivity at various temperatures. Decreased thermal conductivity was observed in the ceramic phases, i.e., reinforcements at 12 wt. % in the ductile phase of TiO_2 with composites of nickel alloy. However, it was concluded that thermal conductivity was affected by temperature content; the reinforcements are listed in Tables 4 to 8.

4.3. Coefficient of Thermal Expansion (CTE). The coefficient of thermal expansion (CTE) addresses the estimation of changes in a material with temperature. The proportion of CTE material in its constituent particles is associated with its bond. It is hard to completely surmise the coefficient of thermal extension of a metal lattice grid, with specific variables influencing it. The pliancy of the material includes the size and position of the fortification, type of guide, dissemination of fortifications, and voids in the composite material. In the current investigation, at various temperatures, the coefficient of thermal expansion was ascribed to

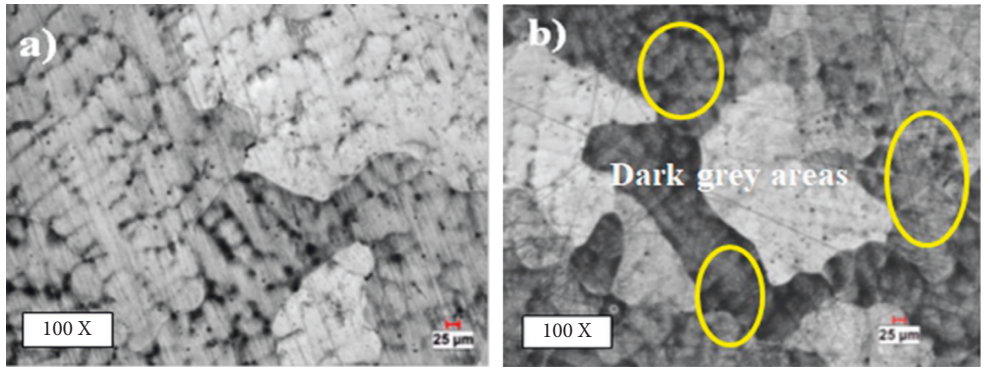

Figure 5: Microstructure images for (a) unreinforced Ni-alloy and (b) Ni-alloy/TiO_2 metal matrix composites.

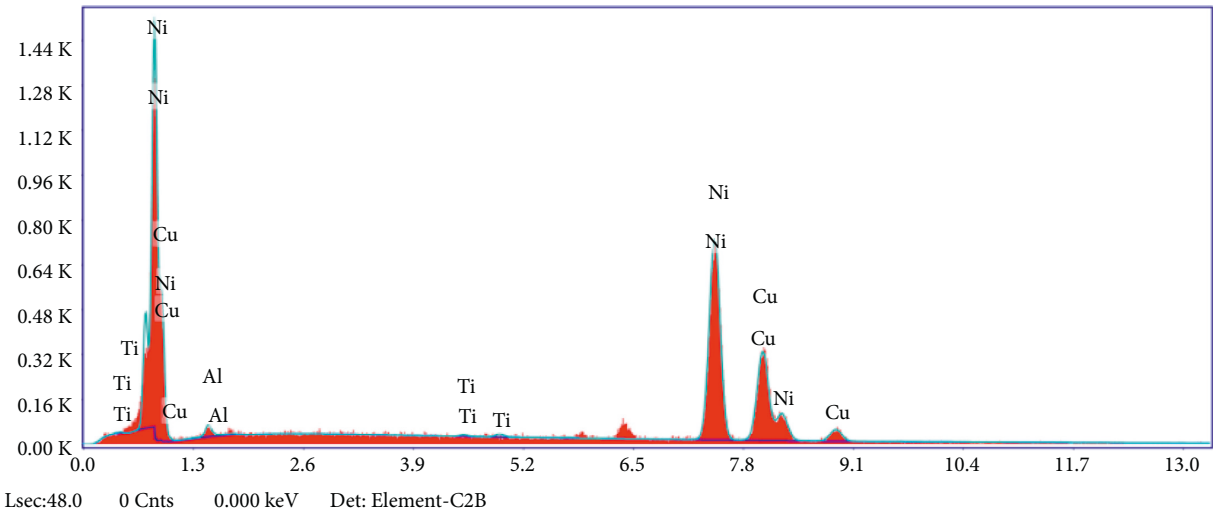

Figure 6: EDX spectrum of Ni-alloy composites (Ni-alloy/TiO_2).

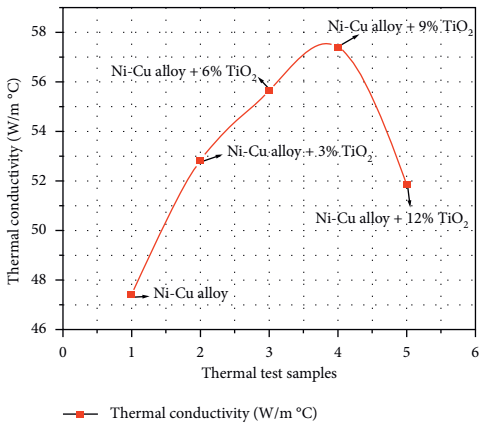

Figure 7: Thermal conductivity of the nanocomposites.

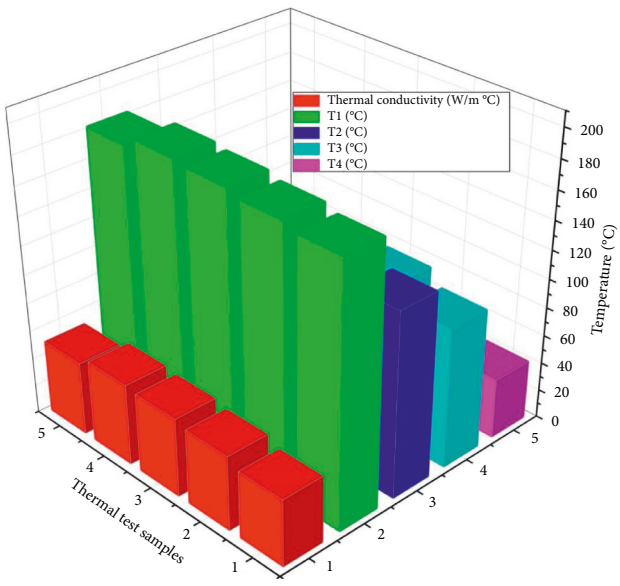

Figure 8: Thermal conductivity at different temperature.

the nickel combination of composites with varying weight percentage of TiO_2 nanoparticulates. The consequence of the experiment was that the coefficient of thermal expansion for both nickel composite material (base metal) and nickel alloy composite with reinforcement material (TiO_2) decreased with increasing temperature as shown in Figure 9. As the reinforcing material increases, CTE gradually drops by a certain temperature to 12% weight of TiO_2. The percentage is caused by ceramic phase (TiO_2) ductile (FCC) matrix (Ni-

Table 4: Thermal conductivity (W/m (℃)) of Ni-Cu alloy (unreinforced) composite.

T_1 (℃)	T_2 (℃)	T_3 (℃)	T_4 (℃)	L_s (mm)	L_r (mm)	K_r (W/m (℃))	K_s (W/m (℃))
79.5	65.3	36.4	24.1	60	60	130	10.559
115.7	72.7	49.3	31.6	60	60	130	18.313
129.4	84.8	58.2	35.9	60	60	130	27.391
140.2	90.7	60.5	36.2	60	60	130	31.244
148	106.8	76.2	37.7	60	60	130	35.045
157.7	112.6	78.1	38.4	60	60	130	39.724
164.1	120.6	87.7	39.4	60	60	130	41.159
173.4	126.4	91.1	40.1	60	60	130	44.618
181.5	129.7	98.5	42.4	60	60	130	47.399

Table 5: Thermal conductivity (W/m (℃)) of Ni-Cu alloy + 3% TiO_2 composite.

T_1 (℃)	T_2 (℃)	T_3 (℃)	T_4 (℃)	L_s (mm)	L_r (mm)	K_r (W/m (℃))	K_s (W/m (℃))
81.2	61.4	38.5	28.6	60	60	130	16.278
108	82.8	45.8	33.7	60	60	130	26.659
118.7	91.1	48	35.1	60	60	130	34.297
134.6	103.4	66.1	37.3	60	60	130	39.036
153.1	109.7	74.3	39.7	60	60	130	43.098
146	118.7	86.3	41.3	60	60	130	46.255
162.6	122	98.7	43.1	60	60	130	48.276
173.2	132.3	101	45.3	60	60	130	50.746
185.2	134.4	109	46.5	60	60	130	52.852

Table 6: Thermal conductivity (W/m ℃)of Ni-Cu + 6% TiO_2 composite.

T_1 (℃)	T_2 (℃)	T_3 (℃)	T_4 (℃)	L_s (mm)	L_r (mm)	K_r (W/m (℃))	K_s (W/m (℃))
98.1	76.6	45.1	29.2	60	60	130	18.468
108.2	85.2	46.8	32.3	60	60	130	25.961
127.2	98.4	50.1	34.4	60	60	130	31.159
137.1	102	62.4	36.7	60	60	130	38.973
145	105.9	74.8	37.9	60	60	130	43.188
157.3	109.8	85.8	39.2	60	60	130	44.222
167.4	114.9	92.5	40.1	60	60	130	49.645
172.5	119.4	96.6	43.2	60	60	130	51.954
181.5	129.7	99.93	45.92	60	60	130	53.453
188.5	136.1	103.23	47.84	60	60	130	55.651

Table 7: Thermal conductivity (W/m (℃)) of Ni-Cu + 9% TiO_2 composite.

T_1 (℃)	T_2 (℃)	T_3 (℃)	T_4 (℃)	L_s (mm)	L_r (mm)	K_r (W/m (℃))	K_s (W/m (℃))
88.8	68.4	39.6	28	60	60	130	20.439
98.9	78.5	44.1	30.4	60	60	130	22.711
118.6	88.7	49.3	32.5	60	60	130	25.831
126.6	95.7	53.3	33.9	60	60	130	30.429
139.1	105.5	57.5	35.1	60	60	130	35.857
148.2	115.6	65.4	37.2	60	60	130	40.477
156.7	120.6	70.8	42.9	60	60	130	47.698
168.3	123.4	85.9	44.7	60	60	130	51.362
174.3	129.8	90.5	45.3	60	60	130	55.897
190.5	139.5	106.71	48.1	60	60	130	57.423

Table 8: Thermal conductivity (W/m ℃) of Ni-Cu + 12% TiO_2 composite.

T_1 (℃)	T_2 (℃)	T_3 (℃)	T_4 (℃)	L_s (mm)	L_r (mm)	K_r (W/m (℃))	K_s (W/m (℃))
93.4	75.7	38.6	26.2	60	60	130	18.756
108.6	84.7	42.2	29.3	60	60	130	25.199
118.1	90.2	46.2	32.3	60	60	130	30.521
127.8	98.1	47.8	34.6	60	60	130	32.572
135.1	106.6	53.3	36.1	60	60	130	35.392
157.6	115.7	63.2	37.9	60	60	130	41.214
168.1	119.1	65.8	39.9	60	60	130	44.136
174.2	121.2	87.1	41.2	60	60	130	47.405
183.5	123.4	90.1	43.5	60	60	130	51.852

Table 9: CTE of the Ni-Cu alloy (unreinforced) composite.

Specimen length (mm)	Specimen temperature (℃)	Delta T (℃)	Rod elongation (mm)	Delta L (mm)	Coefficient of thermal expansion
50	100	0	0.004	0	0
50	125	25	0.009	0.005	6×10^{-6}
50	150	25	0.018	0.007	8×10^{-6}
50	175	25	0.026	0.009	10×10^{-6}
50	200	25	0.039	0.014	13×10^{-6}
50	225	25	0.053	0.016	15×10^{-6}
50	250	25	0.06	0.019	18×10^{-6}

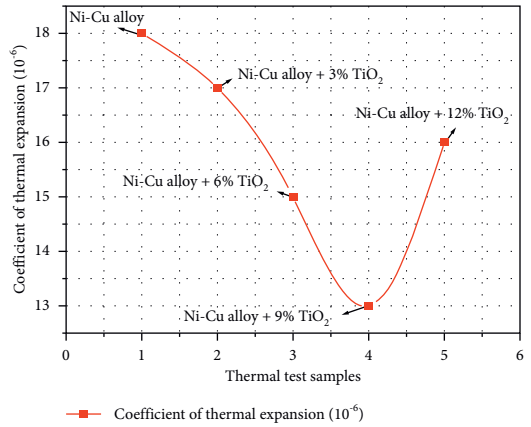

Figure 9: Thermal expansion of the nanocomposites.

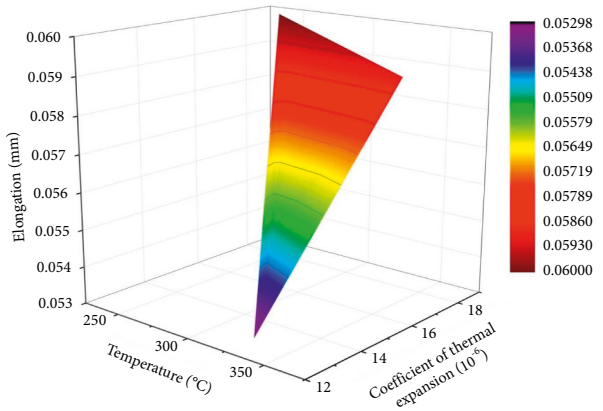

Figure 10: Thermal expansion of the nanocomposites at different temperature.

Table 10: CTE of the Ni-Cu alloy + 3% TiO_2 composite.

Specimen length (mm)	Specimen temperature (℃)	Delta T (℃)	Rod elongation (mm)	Delta L (mm)	Coefficient of thermal expansion
50	125	0	0.008	0	0
50	150	20	0.016	0.006	5×10^{-6}
50	175	25	0.025	0.007	9×10^{-6}
50	200	25	0.035	0.008	11×10^{-6}
50	225	25	0.054	0.013	14×10^{-6}
50	250	25	0.056	0.015	15×10^{-6}
50	275	25	0.059	0.017	17×10^{-6}

Table 11: CTE of the Ni-Cu alloy + 6% TiO_2 composite.

Specimen length (mm)	Specimen temperature (℃)	Delta T (℃)	Rod elongation (mm)	Delta L (mm)	Coefficient of thermal expansion
50	130	0	0.003	0	0
50	150	22	0.012	0.006	3×10^{-6}
50	175	25	0.019	0.009	7×10^{-6}
50	200	25	0.022	0.011	9×10^{-6}
50	225	25	0.031	0.012	10×10^{-6}
50	250	25	0.048	0.013	12×10^{-6}
50	275	25	0.051	0.015	13×10^{-6}
50	300	25	0.055	0.016	15×10^{-6}

Table 12: CTE of the Ni-Cu alloy + 9% TiO_2 composite.

Specimen length (mm)	Specimen temperature (℃)	Delta T (℃)	Rod elongation (mm)	Delta L (mm)	Coefficient of thermal expansion
50	125	0	0.002	0	0
50	150	20	0.008	0.005	2×10^{-6}
50	175	25	0.019	0.006	4×10^{-6}
50	200	25	0.029	0.007	6×10^{-6}
50	225	25	0.035	0.009	7×10^{-6}
50	250	25	0.039	0.01	8×10^{-6}
50	275	25	0.045	0.011	11×10^{-6}
50	300	25	0.051	0.012	12×10^{-6}
50	325	25	0.053	0.014	13×10^{-6}

Table 13: CTE of the Ni-Cu alloy + 12% TiO_2 composite.

Specimen length (mm)	Specimen temperature (℃)	Delta T (℃)	Rod elongation (mm)	Delta L (mm)	Coefficient of thermal expansion
50	100	0	0.001	0	0
50	125	22	0.009	0.003	2×10^{-6}
50	150	25	0.017	0.005	4×10^{-6}
50	175	25	0.021	0.006	7×10^{-6}
50	200	25	0.036	0.011	10×10^{-6}
50	225	25	0.042	0.012	11×10^{-6}
50	250	25	0.046	0.013	12×10^{-6}
50	275	25	0.048	0.014	13×10^{-6}
50	300	25	0.051	0.015	14×10^{-6}
50	325	25	0.054	0.016	15×10^{-6}
50	350	25	0.059	0.017	16×10^{-6}

alloy) reinforcement of 12 weight % TiO_2. CTE value decreases the importance of aggregation and reinforcement clustering (as microstructural observations show). Thus, 12% weight is used to get the least CTE from a composite perspective. Maximum is the ratio of the substitutions applied. Figure 10 further indicates that the maximum CTE (18) is obtained by the nickel alloy and lower CTE (13) for nanocomposites, despite information on reinforcement. Therefore, it is concluded that the nano-MMCs and temperature reinforcement affect the CTE of the developed Ni-alloy MMCs. Tables 9 to 13 show the coefficient of thermal expansion for different temperature.

Adjustment of its material properties is one of the remarkable components of composite material. In its range of application, an important part is the thermal expansion coefficient (CTE) of the composite material. It was found that there was often a micro stress between the matrix and strengthening phases. It is difficult to fully anticipate the thermal expansion of a composite grid given the fact that few elements affect it which include plasticity of the matrix, size and state of reinforcement, support type, reinforcement circulation, and vacuum in the metal network composite. For nickel alloy samples with different weight percentages of reinforcements cast using sand mold techniques, the thermal expansion coefficient is measured in this study. The key findings from the experiment are that the thermal expansion coefficient for both nickel alloy (base metal) and nickel alloy with nanocomposite decreased as temperature increased, and coefficient of thermal expansion drops with an increase in the weight percentage of TiO_2 at 350°C.

5. Conclusion

(i) Microstructure analysis using SEM showed uniform distribution of TiO_2 particulates with the smallest amount of porosities, and agglomeration was observed. Dendritic structure was formed by adding TiO_2.

(ii) Formation of columnar dendrite structure was observed in all metal matrix composite specimens due to faster solidification and density change of the composites by sand casting. The same was also observed in thermal conductivity tests.

(iii) Agglomeration of hard ceramic particles was observed in higher composites, i.e., 12 wt. % TiO_2, due to higher volume ratios and insufficient stirring time and speed.

(iv) EDAX spectral analysis was conducted on the fabricated samples. Other elements, as well as nickel alloy and TiO_2, were found in the results. areThe results of the EDAX spectrum analysis are consistent, showing the presence of additional elements in the fabricated samples.

(v) Thermal conductivity of the nanocomposites increased (17.45%) due to increases in (TiO_2) particulates in the matrix alloy. This was because the hard ceramic particulates in the matrix alloy resisted the higher stiffness of matrix lattice which led to increased thermal conductivity in the nanocomposites.

(vi) CTE of nickel alloy + TiO_2 of 3, 6, 9, and 12 wt. % MMCs decreased by 5.55%, 16.66%, 27%, and 11.11%, respectively, compared to the nickel alloy base metal.

(vii) The inclusion of hard ceramic particles into matrix, the coefficient of thermal expansion for both nickel alloy, and the hybrid composites decreased as temperature increased.

(viii) Reduction in the CTE was identified with an increase in the reward level to 9% of the weight percentage of $TiO_2$and a slight increase to 12% of TiO_2 due to the ceramic reinforcing phase in the ductile matrix alloy (FCC).

Data Availability

The data used to support the findings of this study are included in the article.

Disclosure

This research and publication were performed as part of the employment with Addis Ababa Science and Technology University, Addis Ababa, Ethiopia.

Conflicts of Interest

The authors declare that there are no conflicts of interest regarding the publication of this paper.

Acknowledgments

The authors would like to thank the RL Jalappa Institute of Technology for its excellent support for the submission of this paper.

References

[1] B. Güneş and Ş Erkoç, "Melting and fragmentation of nickel nanoparticles: molecular-dynamics simulations," *International Journal of Modern Physics C*, vol. 11, no. 08, pp. 1567–1580, 2000.

[2] H. P. Meyers and H. P. Myers, *Introductory Solid State Physics*, CRC Press, Boca Raton, FL, USA, 1997.

[3] R. Agarwal, K. VermaVerma, N. K. Agrawal, and R. Singh, "Sensitivity of thermal conductivity for Al2O3 nanofluids," *Experimental Thermal and Fluid Science*, vol. 80, pp. 19–26, 2017.

[4] M. A. Kedzierski, R. Brignoli, K. T. Quine, and J. S. Brown, "Viscosity, density, and thermal conductivity of aluminum oxide and zinc oxide nanolubricants," *International Journal of Refrigeration*, vol. 74, pp. 3–11, 2017.

[5] M. Zielinska, M. Yavorska, M. Porêba, and J. Sieniawski, "Thermal properties of cast nickel based superalloys," *Archives of Materials Science and Engineering*, vol. 44, no. 1, pp. 35–38, 2010.

[6] M. Ravikumar, H. N. Reddappa, and R. Suresh, "Study on mechanical and tribological characterization of Al2O3/SiCp

reinforced aluminum metal matrix composite," *Silicon*, vol. 10, no. 6, pp. 2535–2545, 2018.

[7] G. Purushotham and J. Hemanth, "Influence of fused silica and chills incorporation on corrosion, thermal and chemical composition of ASTM A 494 M grade nickel alloy," *IOP Conference Series: Materials Science and Engineering*, vol. 149, no. 1, Article ID 012042, 2016.

[8] A. T. Nelson, J. T. White, D. A. AnderssonAndersson et al., "Thermal expansion, heat capacity, and thermal conductivity of nickel ferrite (NiFe2O4)," *Journal of the American Ceramic Society*, vol. 97, no. 5, pp. 1559–1565, 2014.

[9] M. Srivastava, A. Srinivasan, and V. K. William Grips, "Influence of zirconia incorporation on the mechanical and chemical properties of Ni-Co alloys," *American Journal of Materials Science*, vol. 1, no. 2, pp. 113–122, 2012.

[10] N. El-Bagoury, M. A. Amin, and Q. Mohsen, "Effect of various heat treatment conditions on microstructure, mechanical properties and corrosion behavior of Ni base superalloys," *International Journal of Electrochemical Science*, vol. 6, no. 12, pp. 6718–6732, 2011.

[11] D. Ulutan and T. Ozel, "Machining induced surface integrity in titanium and nickel alloys: a review," *International Journal of Machine Tools and Manufacture*, vol. 51, no. 3, pp. 250–280, 2011.

[12] T. Trzepiecinski and H. G. Lemu, "Frictional resistances of AMS5599 nickel-based alloy at high pressure conditions," *IOP Conference Series: Materials Science and Engineering*, vol. 381, no. 1, Article ID 012159, 2018.

[13] R. Calin, M. Pul, and Z. O. Pehlivanli, "The effect of reinforcement volume ratio on porosity and thermal conductivity in Al-Mgo composites," *Materials Research*, vol. 15, no. 6, pp. 1057–1063, 2012.

[14] X. D. Liu, J. S. Zhang, X. M. Cao, and H. Zhang, "Finite element simulation of the thermal properties of particulate and continuous network-reinforced metal-matrix composites," *Proceedings of the Institution of Mechanical Engineers - Part B: Journal of Engineering Manufacture*, vol. 219, no. 1, pp. 111–121, 2005.

[15] J. Hemanth and Joel, "Development of nickel alloy reinforced with fused SiO2 chilled composites and evaluation of thermal properties (thermal conductivity & coefficient of thermal expansion) and temperature distribution by finite element analysis (FEA)," *Open Journal of Composite Materials*, vol. 07, no. 05, pp. 251–264, 2017.

[16] S. Cem OKUMUSCem Okumus, S. Aslan, R. Karslioglu, D. Gultekin, and H. Akbulut, "Thermal expansion and thermal conductivity behaviors of Al-Si/SiC/graphite hybrid metal matrix composites (MMCs)," *Materials Science*, vol. 18, no. 4, pp. 341–346, 2012.

[17] S. A. Krishna, T. N. Shridhar, and L. Krishnamurthy, "Microstructural characterization and investigation of thermal conductivity behaviour of Al6061-SiC-Gr hybrid metal matrix composites," *Indian Journal of Engineering and Materials Sciences*, vol. 23, pp. 207–222, 2016.

[18] R. Przeliorz and J. Piatkowski, "Thermo physical properties of nickel-based cast super alloys," *Metallurgy*, vol. 54, no. 3, pp. 543–546, 2015.

[19] A. C. Reddy, "Thermal expansion behavior of aluminum matrix composites reinforced with fused quartz nanoparticles," *National Conference on Advanced Materials and Manufacturing Techniques*, vol. 10, pp. 350–355, 2004.

[20] P. K. Rohatgi, N. Gupta, and S. Alaraj, "Thermal expansion of aluminum-fly ash cenosphere composites synthesized by pressure infiltration technique," *Journal of Composite Materials*, vol. 40, no. 13, pp. 1163–1174, 2006.

[21] M. Ravi KumarRavi Kumar, H. Reddappa, and M. SureshGangadharappa, "Effect of heat treatment on tensile strength of Al7075/Al2O3/SiCp Hybrid composite by stir casting technique," *Materials Today Proceedings*, vol. 5, no. 10, pp. 22460–22465, 2018.

[22] Z. Fattahi, S. A. Sajjadi, A. Babakhani, and F. Saba, "Ni-Cr matrix composites reinforced with nano- and micron-sized surface-modified zirconia: s," *Journal of Alloys and Compounds*, vol. 817, Article ID 152755, 2020.

[23] H. N. Reddappa, K. R. Suresh, H. B. Niranjan, and K. G. Satyanarayana, "Effect of aging on mechanical and wear properties of beryl particulate reinforced metal matrix composites," *Journal of Engineering Science & Technology*, vol. 9, no. 4, pp. 455–462, 2014.

[24] L. C. Davis and B. E. Artz, "Thermal conductivity of metal-matrix composites," *Journal of Applied Physics*, vol. 77, no. 10, pp. 4954–4960, 1995.

[25] A. Matine, N. Boyard, P. Cartraud, G. Legrain, and Y. Jarny, "Thermal properties of composite materials :effective conductivity tensor and edge effects," *Journal of Physics: Conference Series*, vol. 395, no. 1, Article ID 012014, 2012.

[26] R. W. Powell, R. P. Tye, and M. J. Hickman, "The thermal conductivity of nickel," *International Journal of Heat and Mass Transfer*, vol. 8, no. 5, pp. 679–688, 1965.

[27] L. Karikalan, S. Baskar, N. Poyyamozhi, and K. Negash, "Experimental analysis of heat transfer by using nanofluid and impact of thermophysical properties," *Journal of Nanomaterials*, vol. 2022, pp. 1–8, 2022.

[28] J. K. Hulm, "The thermal conductivity of a copper-nickel alloy at low temperatures," *Proceedings of the Physical Society Section B*, vol. 64, no. 3, pp. 207–211, 1951.

[29] M. Selvamuthukumar, B. Harish babu, S. bobba, and N. BaskarJoy, "Investigation on the lubricating behavior of cashew nut shell liquid oil as a renewable and reliable petrochemical product," *Materials Today Proceedings*, vol. 44, no. 2021, pp. 3583–3588, 2021.

[30] S. Baskar, L. Karikalan, V. Vijayan, D. Arunkumar, and K. Sukenraj, "Performance, emission characteristics of compressed ignition engine with alternative fuel," *Materials Today Proceedings*, vol. 37, no. 2021, pp. 995–998, 2021.

[31] S. P. Yuan and P. X. Jiang, "Thermal conductivity of small nickel particles," *International Journal of Thermophysics*, vol. 27, no. 2, pp. 581–595, 2006.